AD-A252 648

Quarterly Letter Report

Growth, Characterization and Device Development in
Monocrystalline Diamond Films

DTIC
S ELECTE
JUL 0 8 1992
A D

R. F. Davis, J. T. Glass, R. J. Nemanich* and R. J. Trew**
B. R. Stoner, J. VanderWeide* and W. Zhu
North Carolina State University
c/o Materials Science and Engineering Department
*Department of Physics
**Electrical and Computer Engineering
Raleigh, NC 27695

June 30, 1992

92-17742

REPORT DOCUMENTATION PAGE

Public reporting burden for this collection of information is estimated to average 1 hour per response, including the time for reviewing instructions, searching existing data sources, gathering and maintaining the data needed, and completing and reviewing the collection of information. Send comments regarding this burden estimate or any other aspect of this collection of information, including suggestions for reducing this burden, to Washington Headquarters Services, Directorate for Information Operations and Reports, 1215 Jefferson Davis Highway, Suite 1204, Arlington, VA 22202-4302, and to the Office of Management and Budget, Paperwork Reduction Project (0704-0188), Washington, DC 20503

1. AGENCY USE ONLY (Leave blank)	2. REPORT DATE June, 1992	3. REPORT TYPE AND DATES COVERED Quarterly Letter 4/1/92–6/30/92

4. TITLE AND SUBTITLE	5. FUNDING NUMBERS
Growth, Characterization and Device Development in Monocrystalline Diamond Films	s400003srr08 1114SS N00179 N66005 4B855
6. AUTHOR(S) Robert F. Davis	

7. PERFORMING ORGANIZATION NAME(S) AND ADDRESS(ES)	8. PERFORMING ORGANIZATION REPORT NUMBER
North Carolina State University Hillsborough Street Raleigh, NC 27695	N00014-90-J-1604

9. SPONSORING/MONITORING AGENCY NAME(S) AND ADDRESS(ES)	10. SPONSORING/MONITORING AGENCY REPORT NUMBER
Department of the Navy Office of the Chief of Naval Research 800 North Quincy Street, Code 1513:CMB Arlington, VA 22217-5000	

11. SUPPLEMENTARY NOTES

12a. DISTRIBUTION/AVAILABILITY STATEMENT	12b. DISTRIBUTION CODE
Approved for Public Release—Distribution Unlimited	

13. ABSTRACT (Maximum 200 words)

Initial bias-enhanced heteroepitaxial nucleation on single crystal SiC has proven to be successful. Transmission electron microscopy (TEM) showed that approximately half of the diamond nuclei were in epitaxial alignment with the SiC substrate. Further TEM both confirmed this epitaxy and also clearly indicated that the nuclei were tilted by several degrees. This tilting was determined to be a result of the high density of inefficient misfit dislocations at the interface. It was found that the tilt component of the misfit dislocations could account for the misorientation in the crystals. It was also suggested that by attempting to grow diamond(114) on SiC(221) the interfacial strain energy and resulting misorientation could be significantly reduced. Photoemission spectroscopy was used to compare the effect of plasma cleaning procedures, and high temperature annealing procedures, on natural type 2B diamond (111) surface. The hydrogen on the diamond surface was desorbed by annealing the diamond to approximately 950°C, and the sharp peak in the photoemission spectra, observed prior to annealing and indicative of a negative electron affinity surface, disappeared. The peak could be recovered by exposing the surface to either plasma generated or hot filament excited mono-atomic hydrogen. Exposure to molecular hydrogen had no effect. These results verify the correlation between the presence of chemisorbed hydrogen on the diamond (111) surface and a negative electron affinity of that surface. Photoemission after argon plasma exposure of the H-terminated surface showed that the negative electron affinity was removed. This result indicated that exposure to an RF induced argon plasma can also be used to remove the hydrogen from the diamond (111) surface, but at a considerably lower temperature.

14. SUBJECT TERMS diamond thin films, silicon carbide, heteroepitaxial nucleation, misfit dislocations, interfacial strain energy, plasma cleaning, negative electron affinity, atomic hydrogen, argon plasma, uv photoemission			15. NUMBER OF PAGES 12
			16. PRICE CODE

17. SECURITY CLASSIFICATION OF REPORT UNCLAS	18. SECURITY CLASSIFICATION OF THIS PAGE UNCLAS	19. SECURITY CLASSIFICATION OF ABSTRACT UNCLAS	20. LIMITATION OF ABSTRACT SAR

Table of Contents

Accesion For

NTIS CRA&I		☑
DTIC TAB		☐
Unannounced		☐
Justification		

By
Distribution /

Availability Codes

Dist	Avail and / or Special
A-1	

I. Introduction

Diamond as a semiconductor in high-frequency, high-power transistors has unique advantages and disadvantages. Two advantages of diamond over other semiconductors used for high-frequency, high-power devices are its high thermal conductivity and high electric-field breakdown. The high thermal conductivity allows for higher power dissipation over similar devices made in Si or GaAs, and the higher electric field breakdown makes possible the production of substantially higher power, higher frequency devices than can be made with other commonly used semi-conductors.

In general, the use of bulk crystals severely limits the potential semiconductor applications of diamond. Among several problems typical for this approach are the difficulty of doping the bulk crystals, device integration problems, high cost and low area of such substrates. In principal, these problems can be alleviated via the availability of chemically vapor deposited (CVD) diamond films. Recent studies have shown that CVD diamond films have thermally activated conductivity with activation energies similar to crystalline diamonds with comparable doping levels. Acceptor doping via the gas phase is also possible during activated CVD growth by the addition of diborane to the primary gas stream.

The recently developed activated CVD methods have made feasible the growth of polycrystalline diamond thin films on many non-diamond substrates and the growth of single crystal thin films on diamond substrates. More specifically, single crystal epitaxial films have been grown on the {100} faces of natural and high pressure/high temperature synthetic crystals. Crystallographic perfection of these homoepitaxial films is comparable to that of natural diamond crystals. However, routes to the achievement of rapid nucleation on foreign substrates and heteroepitaxy on one or more of these substrates has proven more difficult to achieve. This area of study has been a principal focus of the research of this contract.

At present, the feasibility of diamond electronics has been demonstrated with several simple experimental devices, while the development of a true diamond-based semiconductor materials technology has several barriers which a host of investigators are struggling to surmount. It is in this latter regime of investigation that the research described in this report has and continues to address.

The principal vectors of the research in this reporting period have been (1) the determination of the reason for the crystallographic tilting of the diamond films nucleated on beta-SiC substrates and (2) the determination of the effort of chemisorbed hydrogen on the diamond (111) surface on the presence of a negative electron affinity.

The following subsections detail the experimental procedures for each of the aforementioned studies, discuss the results and provide conclusions and references for these studies. Note that each major section is self-contained with its own figures, tables and references.

II. Analysis of the Diamond/SiC Interface via Cross Sectional Transmission Electron Microscopy

A. Introduction

It has been shown in a previous publication that textured diamond may be nucleated on beta-SiC [1]. This locally epitaxial relationship between the diamond and SiC was confirmed by high resolution cross-sectional TEM. Figure 1 shows an XTEM micrograph of the diamond on SiC interface. In this <110> projection, the diamond $(1\bar{1}1)$ planes are shown to be continuous across the interface. A 4–6° tilting of the diamond $(1\bar{1}1)$ planes towards the $<\bar{1}10>$ direction is also evident. The large fringes near the interface are Moiré fringes, indicating that there is overlap between the diamond and SiC in this region. Since the Moiré fringes are very sensitive to the misorientation between two overlapping lattices, they provide an excellent measure of the tilt boundary at the interface.
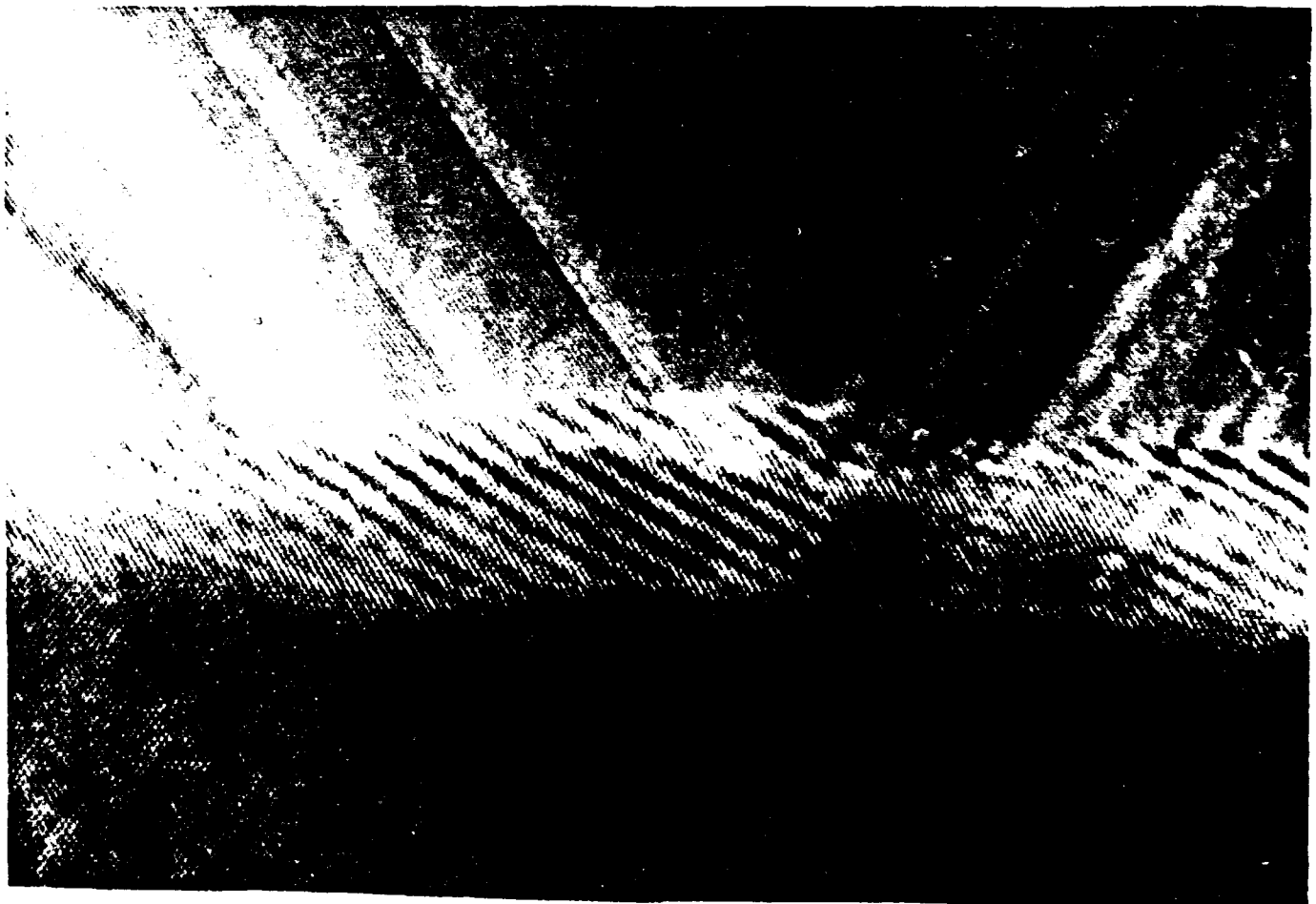
Figure 1.   High resolution transmission electron micrograph of the diamond/SiC interface. The largely spaced lines at the interface are Moiré fringes, representing a slight overlap between diamond and SiC.

2

It is also important to note that there does not appear to be an interfacial layer between the diamond and SiC. In a previous study of bias-enhanced diamond nucleation on silicon [2], an amorphous interfacial layer was observed. In that particular study the bias-pretreatment was performed for 1 hr; in the present study, the duration was 30 min. By reducing the pretreatment time to 30 min, it is believed that nucleation was enhanced significantly, over that for an untreated surface, but, without damaging this surface or depositing on it an amorphous layer.

B. Results

It was mentioned above that a tilt boundary developed between the diamond and SiC substrate. A misorientation of this nature is not desirable, since it results in low-angle grain boundaries between the various diamond grains once they grow into a complete film. A high density of low angle grain boundaries will degrade the electrical properties of the resulting diamond film, thus the mechanism for the formation of this tilt boundary is of great interest. The possible mechanisms considered are; (i) tilting of the diamond lattice to expose a high index plane, thus reducing the lattice mismatch and the resulting interfacial strain energy, and (ii) a tilt boundary resulting from a high density of inefficient misfit dislocations at the interface.

The first mechanism is shown schematically in Figure 2. The amount of misfit between two dissimilar lattices may be reduced by tilting the smaller lattice to expose a higher index plane to the interface. As illustrated in this figure, the SiC and diamond have lattice parameters of a_0 and a_1 respectively. By tilting through an angle, α, the smaller lattice may be made to match that of the larger one in this simple two-dimensional model. When all of the mismatch is accounted for by this rotation, resulting in no interfacial strain, the tilt angle may be calculated from simple geometry as follows;
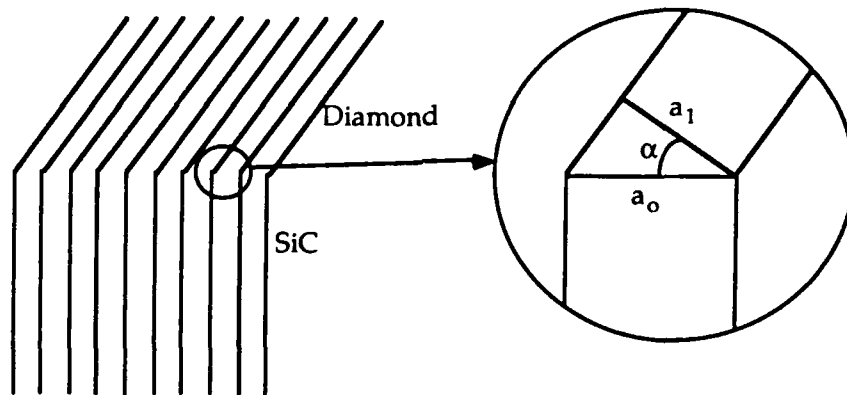
$$\cos(\alpha) = a_1/a_0. \qquad (1)$$

Figure 2.   Schematic representation of a tilt boundary, exposing a high index diamond plane on (100) SiC.

For diamond on β-SiC, the one-dimensional rotation angle (α) resulting in a minimum strain energy would be;

$$\alpha = \cos^{-1}(3.57/4.36) = 35°.$$

The rotation observed in the TEM micrographs was approximately 5°, which will only offset a lattice mismatch of 0.4%. For diamond on SiC the lattice mismatch is roughly 20%, which implies that a 5° rotation will only reduce the total interfacial elastic strain energy by approximately 2%. It is therefore unlikely that the observed misorientation is a result of this type of interfacial lattice rotation mechanism.

The second possibility is that the tilt may be caused by the high number of misfit dislocations at the interface. It has been shown in previous work that the misfit dislocations in diamond and zincblend lattices consist mostly of the 60° mixed type [3, 4, 5]. These 60°-type dislocations may be resolved into both a tilt (b_1) and misfit (b_2) component, as discussed by Olsen and Ettenberg [6], and shown schematically in Figure 3. Figure 4 shows also how a tilt boundary may result from an array of dislocations running parallel to the interface. A partial component of the 60° dislocation will be parallel to the interface and thus result in a low angle grain boundary. The magnitude of the tilt resulting from an array of pure horizontal dislocations may be calculated from the relationship [7];

$$\sin(\alpha) = |b|/D. \tag{2}$$

Where b is the Burgers vector and D is the dislocation spacing.

60 °
Dislocation
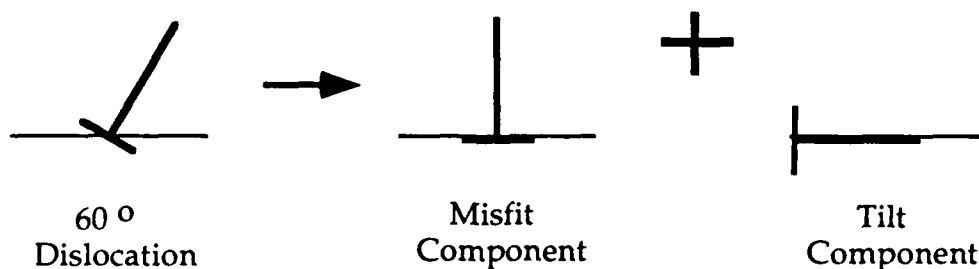
Misfit
Component

Tilt
Component

Figure 3.   Schematic representation of how a 60° mixed-type dislocation may be resolved into both a misfit and a tilt component.
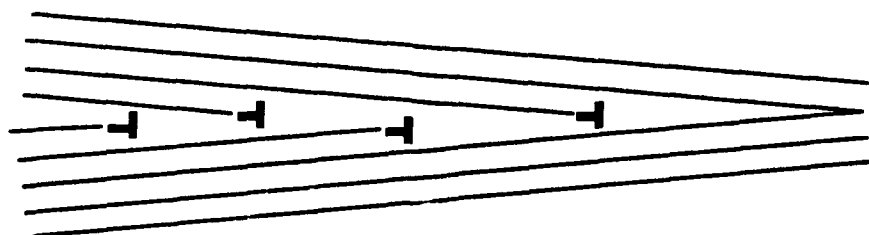

Figure 4.   Schematic representation of a low-angle grain boundary, caused by an array of edge-type dislocations with Burgers vectors running normal to the interface.

On a (001) oriented substrate, a mixed interfacial dislocation along an <011> direction will have a Burgers vector, b = <101>, inclined 45° to the interface [6]. The tilt component (b_1) of this Burgers vector will be in the <001> direction, with b_1 = 0.707b. If one then measures the dislocation spacing from the high resolution XTEM in Figure 1, the misorientation(a) may be calculated from equation (2) as;

$$\sin(\alpha) = 0.707 \, |b| / D.$$

However, the quantity $|b|/D$ is simply the dislocation density (ρ). From Figure 1, there is on average 1 misfit dislocation every 7 lattice planes, which translates to a dislocation density of 0.14. With this dislocation density the misorientation angle (α) is calculated to be;

$$\alpha = \sin^{-1}(0.707\rho) = 5.8°, \tag{3}$$

which is in very good agreement with the measured misorientation of 5°. This suggests that the high density of 60° misfit dislocations is largely responsible for the observed rotation of the diamond grains.

C. Discussion

It is of interest to point out that the measured misfit dislocation density is slightly lower than that expected for a 20% lattice mismatch. If all of the interfacial strain energy was absorbed via perfect edge-type misfit dislocations, then one would expect on average, 1 dislocation for every 5 lattice planes. For the 60° -type dislocations the misfit component (b_2) will be along the interface in the <1$\bar{1}$0> direction with $|b_2| = |b|/2$. Therefore the mixed dislocations are only half as efficient in relieving the misfit strain as the perfect edge-type, and thus the predicted dislocation density increases to $\rho = 0.4$, or an average of 1 every 2.5 lattice planes. This implies that the diamond nuclei observed in this study are still highly strained near the interface. If the interfacial strain were minimized by a dislocation density of 0.4, the predicted rotation, calculated via equation (3) would be approximately 16° instead of the observed 5°.

A random rotation of this magnitude between the various diamond grains no longer constitutes a low angle grain boundary and should effectively result in a polycrystalline diamond film. It appears to be fortunate therefore that the interfacial strain is not minimized via the incorporation of misfit dislocations that would hence result in large distribution of crystal-misorientations. Of interest is a recent proposal by Zhu *et. al* [8], for the epitaxial growth of diamond(114) on SiC(221). This epitaxial configuration should theoretically result in an elastic interfacial strain energy that is half that of the D(100) on SiC(100) system which has been reported here. Based on the logic presented above, if the misfit strain energy were to be minimized via the incorporation of misfit dislocations for this system, the maximum misorientation would be only approximately 8° versus 16° for the diamond(100) on SiC(100) case. If the interface were to remain partially strained, as in the that observed via XTEM, then it

is plausible that epitaxial films with low-angle grain boundaries misoriented by less than 5° could be achieved.

D. Summary

Initial bias-enhanced heteroepitaxial nucleation on single crystal SiC has proven to be successful. Transmission electron microscopy (TEM) showed that approximately half of the diamond nuclei were in epitaxial alignment with the SiC substrate. Further TEM both confirmed this epitaxy and also clearly indicated that the nuclei were tilted by several degrees. This tilting was determined to be a result of the high density of inefficient misfit dislocations at the interface. It was found that the tilt component of the misfit dislocations could account for the misorientation in the crystals. It was also suggested that by attempting to grow diamond(114) on SiC(221) the interfacial strain energy and resulting misorientation could be significantly reduced.

E. References

1. B. R. Stoner and J. T. Glass, Appl. Phys. Lett. **60**, 698 (1992).
2. B. R. Stoner, G.-H. M. Ma, S. D. Wolter, and J. T. Glass, Phys. Rev. B in press (1992).
3. P. M. J. Maree, J. C. Barbour, J. F.v.d. Veen, K. L. Kavanagh, C. W. T. Bulle-Lieuwma, and M. P. A. Viegers, J. Appl. Phys. **62**, 4413 (1987).
4. R. J. Matyi, J. W. Lee, and H. F. Schaake, J. Electronic Mater. **17**, 87 (1988).
5. R. J. Matyi, H. F. Schaake, D. G. Deppe, and J. N. Holonyak, **1**, 195 (The Electrochemical Society, Chicago, Il, 1988).
6. G. H. Olsen, and M. Ettenberg, in *Crystal Growth: Theory and Techniques*, C. H. L. Goodman, ed. (Plenum Press, New York, 1978).
7. D. A. Porter, and K. E. Easterling, *Phase Transformations in Matals and Alloys* (Van Nostrand Reinhold Co. Ltd., Berkshire, 1988).
8. W. Zhu, X. H. Wang, B. R. Stoner, H. S. Kong, M. Braun, G.-H. M. Ma, and J. T. Glass, to be submitted to Phys. Rev. B. (1992).

III. Effects of Hydrogen and Argon Plasma Exposure on the Diamond (111) Surface

A. Introduction

Diamond has excellent properties to be used as a high speed, high temperature semiconductor. With the advent of low temperature, low pressure growth of diamond it has the possibility to become an economically viable semiconductor. In the current semiconductor technologies surface preparation is an important aspect of device fabrication and it will certainly become an issue in the fabrication of diamond devices. Currently there are many different *ex situ* cleaning methods in use. These are generally a combination of polishing the diamond, followed by a solvent rinse or an acid etch. Diamond (111) surfaces that have been polished and chemically cleaned are typically hydrogen terminated [1-3] and have been shown to exhibit a negative electron affinity [1,2]. The hydrogen can be desorbed from the surface by heating the diamond *in situ* to a temperature above 950°C. After the hydrogen has been removed the negative electron affinity effect is removed. It has been shown that the negative electron affinity effect only reappears upon exposure to mono-atomic hydrogen, whereas exposure to molecular hydrogen has no effect on the negative electron affinity [1]. This confirms the relation between chemisorbed hydrogen and the negative electron affinity on the diamond (111) surface. In this paper we confirm the above described experimental result, and use it to show that a low temperature method, based on a RF induced argon plasma, can also be used to remove hydrogen from the diamond (111) surface.

Angle resolved ultra-violet photoemission spectroscopy was used to analyze the surface. The presence of a negative electron affinity can be easily verified by the presence of a sharp peak at the low energy end of the spectrum. This peak is due to emission of secondary electrons that are quasi-thermalized to the edge of the conduction band [4].

B. Experimental Procedure

The diamond substrates used in this study were a $3 \times 3 \times 0.5$ mm^3 IIB (p-type) natural diamond with a (111) surface orientation and a 1.6 Ω cm resistivity. The substrates were polished with 0.1 μm diamond grit and cleaned in a chromic acid solution before loading. The diamond was sutured on to a 2.5mm thick molybdenum disk with tantalum wire. In the first set of experiments the diamond was heated radiatively from the back of the molybdenum disk. Using a thermocouple the temperature was measured at the back of the disk. In order to completely desorb hydrogen the disk had to be heated twice to 1100°C for about 10 minutes. Using an optical pyrometer it was found that this corresponds to temperature of about 950°C on the front side of the disk. The diamond was then exposed to 10^{-6} Torr molecular hydrogen for 5 minutes. Which was followed by 3 min in 10^{-6} Torr molecular hydrogen with a hot (1600°C) filament present. This was done to create mono-atomic hydrogen. The amount of dissociated

7

hydrogen actually present, however, was not determined. In the final step the hydrogen was desorbed again by a 950°C anneal. After every step in the process the sample was examined with ultra-violet photoemission spectroscopy.

In a second set of experiments the diamond was exposed to a remote, RF induced, hydrogen plasma, followed by an argon plasma and a hydrogen plasma. While exposed to either plasma the sample was heated in a similar fashion as described above to about 350°C. The gas flow was kept at 10 sccm while the pressure was held at 14 mTorr. The power to the plasma was 20W. The samples were exposed for a duration of 10 minutes. A more extensive description of the plasma chamber can be found in the literature [5]. After exposure to the plasma the sample was transferred under UHV conditions to the angle resolved photoemission chamber for analysis.

The photoemission was excited with 21.21 eV He(I) radiation, and the data presented here was obtained with a 50 mm hemispherical analyzer with an angular resolution of 2° and an energy resolution of 0.2 eV. When necessary a small bias voltage, less than 1V, was applied to the sample during the measurements to overcome the work function of the analyzer. This was done to include the low energy electrons, which show the negative electron affinity effect, in the spectrum. The presence of a negative electron affinity can be clearly seen by a sharp peak in the low energy end of the spectrum

C. Results and Discussion

In our experiment we started by verifying the experiment of Pate [1] in which the relation between the negative electron affinity effect and the presence of hydrogen on the surface is established. Photoemission spectra from the diamond before and after thermal desorption of the hydrogen are shown in Figure 1. The negative electron affinity of the surface, which results in the sharp peak at the low energy end of the spectrum, has clearly been removed from the surface. Since the annealing temperature used to obtain the effect is the same as the reported temperature for the desorption of hydrogen, this suggest that hydrogen on the surface plays a role in the negative electron affinity effect. The spectra of the diamond before and after annealing, are followed by spectra from the diamond after exposure to molecular and mono-atomic hydrogen. As is shown in Figure 1, the molecular hydrogen has no effect on the electron affinity of the surface. The mono-atomic hydrogen, however, returned the surface to a negative electron affinity state. The fact that exposure to mono-atomic hydrogen causes the surface to exhibit a negative electron affinity confirms that the hydrogen is associated with the negative electron affinity. The difference between the results after exposure to molecular and mono-atomic hydrogen suggest that the hydrogen has to be chemically bonded to the surface. The series is concluded by a spectrum of the diamond after another high temperature anneal, which shows that the cycle is repeatable.

The Effect of Hydrogen on Diamond (111)

Negative electron affinity peak

He(I) radiation normal emission

After loading and 650°C anneal

After 950°C

Exposure to H2

Exposure to H

After 950°C

arbitrary units

-18 -16 -14 -12 -10 -8 -6 -4 -2 Ef
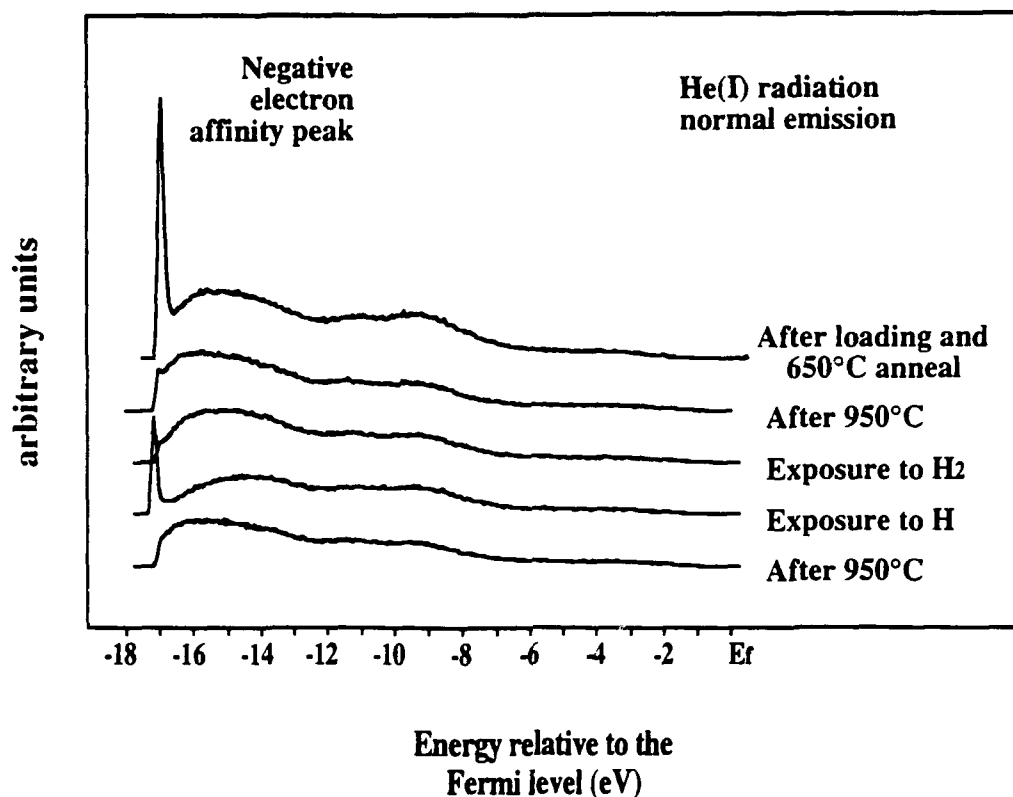
Energy relative to the Fermi level (eV)

Figure 1. Photoemission spectra of diamond (111). The as loaded spectrum (top) shows the presence of a negative electron affinity, causing the sharp peak (A). After a 950°C anneal the peak is gone, indicating the absence of a negative electron affinity. No significant changes occur after exposure to 5 Langmuir molecular hydrogen. After exposure to mono-atomic hydrogen however the negative electron affinity returns. The bottom spectrum, after another 950°C anneal, shows that the cycle can be repeated.

In a second series of experiments the diamond (111) was exposed to a hydrogen plasma after loading. The resulting spectrum in Figure 2 reveals the presence of a negative electron affinity. After a subsequent exposure to an argon plasma, however, the sharp peak that is associated with a negative electron affinity, was absent. Since the negative electron affinity is associated with the presence of hydrogen on the surface we conclude that the argon plasma removed the hydrogen from the surface. Exposure to another hydrogen plasma causes the negative electron affinity effect to reappear. This is to be expected in light of the first experiment where exposure to mono-atomic hydrogen also caused the negative electron affinity to reappear.

D. Conclusions

We have repeated and confirmed the experiment done by Pate et al. that showed that the observed negative electron affinity of the diamond (111) surface is related to hydrogen chemisorbed to the surface. It has been established that hydrogen plasma exposure is efficient

9

Diamond (111) after Argon and Hydrogen plasma

He(I) radiation
normal emission

After H2
plasma

After Ar
plasma

After H2
plasma

-16 -14 -12 -10 -8 -6 -4 -2 Ef
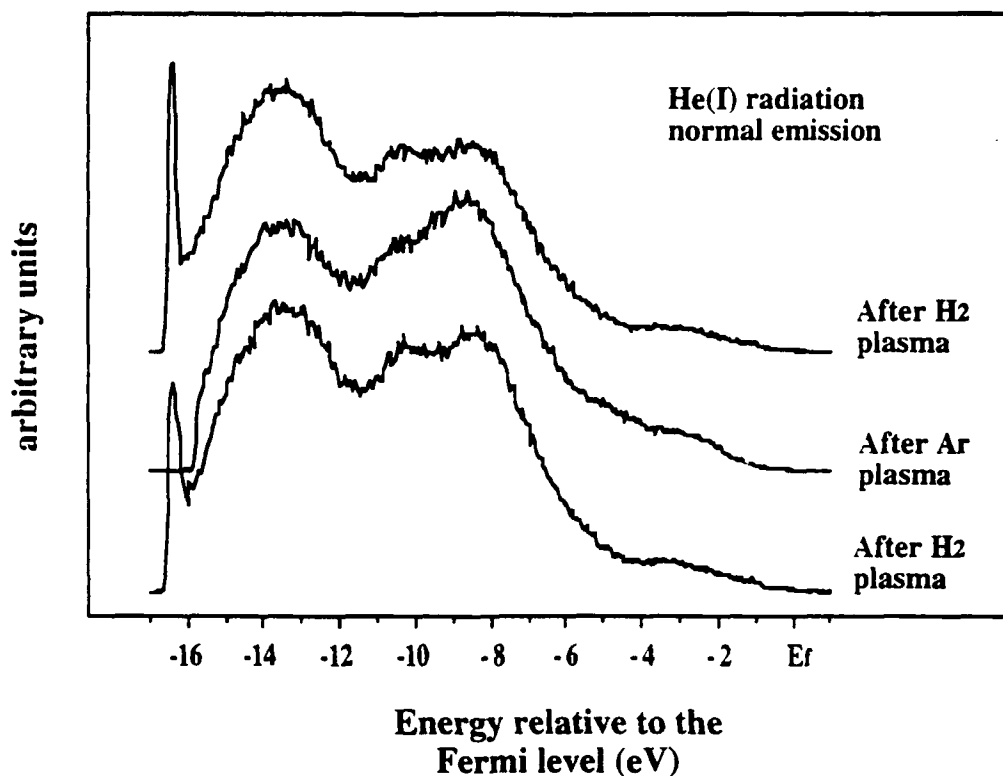
**Energy relative to the
Fermi level (eV)**

Figure 2.   Photoemission spectra of diamond (111) after exposure to: from bottom to top, an hydrogen plasma, an argon plasma and a hydrogen plasma. The diamond was heated to approximately 350°C during each exposure. The spectrum after the first hydrogen plasma shows a sharp peak, due to the negative electron affinity of the surface. In the second spectrum, after argon plasma exposure, the peak is absent, indicating a positive or zero electron affinity. Since the negative electron affinity is linked to the presence of hydrogen, this suggests that hydrogen can be removed from the diamond (111) surface by an argon plasma. In the third spectrum the negative electron affinity is seen to reappear, after exposure to another hydrogen plasma.

at producing an H-termination of the (111) surface resulting in a negative electron affinity. The temperature needed to desorb the hydrogen, is of the order of 950°C. We have used the relation between the negative electron affinity and the presence of hydrogen on the surface to show that an RF induced argon plasma can be used to induce a surface which does not exhibit a negative electron affinity, and it is proposed that the process results in the removal of the hydrogen from the diamond surface. In this process the diamond was heated to ~350°C, which is considerably lower than the temperature needed for thermal desorption.

E. Future Research Plans and Goals

The main focus of our research is to explore Schottky barrier formation for metals on diamond. We have completed the initial stages of work on the titanium-diamond (111) interface [6,7], and are about to finish the titanium-diamond (100) interface. One of the interesting

results from the experiments on the titanium-diamond(111) interface was the fact that a thin layer of titanium can lower the work function of the diamond (111) surface sufficiently to create a negative electron affinity surface. A model, linking the work function of titanium and the Schottky barrier height of the titanium-diamond(111) interface, was proposed to explain this result [7]. A similar effect was observed on the diamond (100) surface, which is something that we plan to investigate further.

In the beginning of this year we brought a new transfer system on-line, which allows us to transfer under UHV conditions to a number of chambers, notably our MBE system. The MBE is currently loaded with nickel and hafnium which are the next metals that will be investigated. We intend to determine the Schottky barrier height of these metals with the diamond (111) and (100) surfaces. We will also be looking at negative electron affinity effects of these metals on the diamond surfaces in order to expand our model to other metals.

On the subject of cleaning and surface preparation of diamond, we intent to finalize for publication the results described above. We are currently initiating a collaboration with a theory group in the physics department. Our aim is to do cluster calculations on the charge distribution of a hydrogen terminated diamond (111) surface to determine the sign and magnitude of the surface dipole layer. This would indicate how the presence of chemisorbed hydrogen can lower the work function of the surface.

F. References

1. B. B. Pate, M. H. Hecht, C. Binns, I. Lindau, W. E. Spicer, J. Vac. Sci. Technol., 21:364, (1982).
2. F. J. Himpsel, J. A. Knapp, J. A. VanVechten, D. E. Eastman, Phys. Rev. **B20**, 624 (1979).
3   A. V. Hamza, G. D. Kubiak, R. H. Stulen, Surf. Sci. Lett. **206**, L833 (1988).
4. C. Piaget, J. Vannimenus, P. Saget, J. Appl. Phys. **48**, 3901 (1977).
5. Jeawon Cho, T. P, Schneider, J. van der Weide, Hyeontag Jeon, R. J. Nemanich, Appl. Phys Lett, **59**, 1995 (1991).
6. J. van der Weide, R. J. Nemanich, *Proceedings of the First International Conference on the Applications of Diamond Films and Related Materials*, edited by Y. Tzeng, M. Yoshikawa, M. Murakawa, A. Feldman, (Elsevier, New York, 1991), p. 359.
7. J. van der Weide, R. J. Nemanich, J. Vac. Sci. Technol. **B10**(4), (in press) 1992.

IV. Distribution List

Number of Copies

Mr. Max Yoder   3
Office of Naval Research
Electronics Division, Code: 1114SS
800 N. Quincy Street
Arlington, VA 22217-5000

Administrative Contracting Officer   1
Office of Naval Research
Resident Representative
The Ohio State University Research Center
1314 Kinnear Road
Columbus, OH 43212-1194

Director   1
Naval Research Laboratory
ATTN: Code 2627
Washington, DC 20375

Defense Technical Information Center   4
Bldg. 5, Cameron Station
Alexandria, VA 22314